Regular Article

PHYSICAL CHEMISTRY RESEARCH
Published by the
Iranian Chemical Society
www.physchemres.org
info@physchemres.org

***Phys. Chem. Res.**, Vol. 7, No. 1, 111-130, March 2019*
DOI: 10.22036/pcr.2018.139119.1503

Minimum Miscibility Pressure Using the Multiple Mixing-cell Combined with the PC-SAFT Equation of State

Y. Khayyat, F. Esmaeilzadeh* and A. Rasoolzadeh

[a]*Department of Chemical and Petroleum Engineering, School of Chemical and Petroleum Engineering, Enhanced Oil and Gas Recovery Institute, Advanced Research Group for Gas Condensate Recovery, Shiraz University, Shiraz, Iran, 7134851154*

(Received 4 July 2018, Accepted 25 November 2018)

The minimum miscibility pressure (MMP) is one of the crucial and substantial parameters in the gas injection projects for enhanced oil recovery (EOR). This parameter indicates the minimum pressure at constant temperature and composition conditions for reaching 100 percent of the oil production recovery, which leads to a huge economic income. Therefore, an inaccurate prediction of the MMP may lead to increase the costs of oil production. Among the various methods for prediction of the MMP: slim-tube experiment, slim-tube simulation techniques and their simplified cell-to-cell could be considered as the most accurate methods. Although the experimental methods for calculation of the MMP take into account the real crude oil, but they are always expensive; therefore, thermodynamic simulation is a better way for the estimation of this parameter. Indeed, the analytical methods are fast and some of them like multiple mixing-cell method used in this study lead to the reliable results and often show good agreements with the experimental methods. A combination of multiple mixing-cell model proposed by Ahmadi-Johns and pressure-temperature (P-T) flash calculations including the PC-SAFT equation of state (EoS), and the cubic equations of state of Peng-Robinson (PR) and Esmaeilzadeh-Roshanfekr (ER) were used in this work for the prediction of MMP. The overall AAD% of the PC-SAFT, PR and ER EoSs were 3.49%, 6.32% and 7.59%, respectively. It is concluded that the SAFT EoS can decrease the AAD of MMP calculation by about 50%.

Keywords: Minimum miscibility pressure, Enhanced oil recovery, PC-SAFT, Gas injection

INTRODUCTION

Nowadays, fossil fuel resources are the major sources of the world energy. Since these sources of energy are non-renewable, the maximum recovery efficiency of these resources must be reached. Miscible gas injection into the oil reservoir is a widely-used, desired method among the various enhanced oil recovery (EOR) methods that is growing fast in the world. The minimum miscibility pressure (MMP) is one of the most significant and substantial parameters in the enhanced oil recovery. MMP is the pressure by which the maximum recovery would be achieved [1-3]. There are various experimental methods for measuring the MMP including sand-packed-slim tube, multiple contact method (MCM), rising bubble apparatus (RBA) and vanishing interfacial tension (VIT) method. The slim tube laboratory test is a widely-used and applicable method for measuring the MMP. Although the slim tube is the best method to estimate the MMP, it has some deficiencies such as lack of high precision, being time-consuming, and high cost. . The second method is the MCM which can calculate the MMP with a good precision when the mechanism is condensation or vaporization. When the mechanism is the combination of condensation/ vaporization, the MMP would not be precisely measured. The MCM is faster and cheaper than the slim tube method. The third method is the RBA which can measure the MMP very fast, but it stands for the forward-contacting miscibility process, hence, it is unable to estimate the MMP for a backward or combined contact mechanism with a good

*Corresponding authors. E-mail: esmaeil@shirazu.ac.ir

accuracy. The VIT experiment can also be used for measuring the MMP in the miscible gas injection method. The basis of this method is the measurement of the interfacial tension between the oil and injected gas at constant temperatures and various pressures. In this method, the MMP is defined experimentally through the measurement of a decrease in the gas-oil interfacial tension (IFT) by increasing the pressure and extrapolating to the zero value [4-10]. In addition to the aforementioned experimental methods, there are several correlations to estimate the MMP. All of these correlations are developed by fitting their constants using the experimental data within a limited range of operating conditions. A slight change in the reservoir condition leads to higher levels of error in the estimated MMPs by these correlations [11-14]. The aforementioned drawbacks of both experimental and empirical methods lead to the development of some analytical methods for MMP estimation. There exist three primary analytical methods to calculate the MMP: 1- calculation of the MMP by the method of characteristics (MOC), 2- calculation of the MMP by slim tube compositional simulation, 3- calculation of the MMP by multicontact mixing cell methods. In this paper, the focus is on the third category, which is the multicontact mixing cell model. The most important method for calculation of the MMP is the mixing-cell method. In this method, mixing and continuous contact of oil and gas lead to different equilibrium compositions. The basis of all the single and multiple mixing cell methods is mixing of gas and oil analytically in several repetitious contacts that leads to the new equilibrium compositions. The multi-contact mixing cell method could calculate an accurate MMP for both condensation/vaporization mechanisms [15]. Esmaeilzadeh and Roshanfekr [16,17] proposed a model to calculate the MMP by a combination of the Wang single simulation method [1] and Esmaeilzadeh-Roshanfekr (ER) equation of state (EoS) for gas condensate reservoirs. They also compared the results of the ER EoS with the Peng-Robinson [18,19], Patel-Teja [20] and Patel-Teja-Valderrama [21] equations of state using some experimental data. Calculated MMPs were in a good agreement with the experimental data, indicating the accuracy of their model. In the case of multiple mixing cell method, Jaubert *et al.* presented the mixing cell algorithms in which they applied specific amounts of gas and excess oil from one cell to the other one. They concluded that dispersion can have major effects on their method [22,23]. Zhao *et al*. offered a complicated multiple mixing cell method to calculate the MMP [24,25]. Ahmadi *et al.* presented a fast multiple mixing cell method to calculate the MMP for the systems in which the number of components has no impact on the MMP calculation. Their mixing cell method was started with two cells and the number of cells was increased until the favorite precision in the key tie lines gained. The MMP was determined on the basis of the pressure at which the first key tie line length reached zero [26].

Since, the most of hydrocarbon mixtures contain nonpolar components, the simple EoS can predict the phase behavior of a hydrocarbon mixture. However, for the case of more complicated systems, a precise EoS should be used. To address the complexity of oil and its products, the perturbed-chain statistical associating fluid theory (PC-SAFT) EoS was proposed. This paper employed the PC-SAFT EoS to investigate the impact of pressure, temperature and composition on the stability and phase behavior of the gas condensate and crude oil required for the calculation of the MMP. The SAFT EoS, which is a multifunction molecular model, is able to consider the effect of molecular shape, weak van der Waals forces, polar forces and association of materials on the thermodynamic properties, stability and phase behavior of all the fluids [27-32]. In this study, a combination of the PC-SAFT with rigorous multiple mixing-cell method, extended by Ahmadi and Johns [33], is applied to calculate the MMP. Thereafter, the results of this method are compared with those obtained by the Esmaeilzadeh-Roshanfekr (ER), and Peng-Robinson (PR) [18,19] equations of state. The proposed method can effectively be used for the calculation of MMP in a multicomponent system with any number of components. Moreover, in spite of Ahmadi and Johns method, our proposed method does not need to gain the whole of the key tie lines and can be simply satisfied by tracking only the shortest one [15,34-35].

THEORY

Cubic and Molecular Equations of State

An EoS is needed for the phase equilibrium calculations.

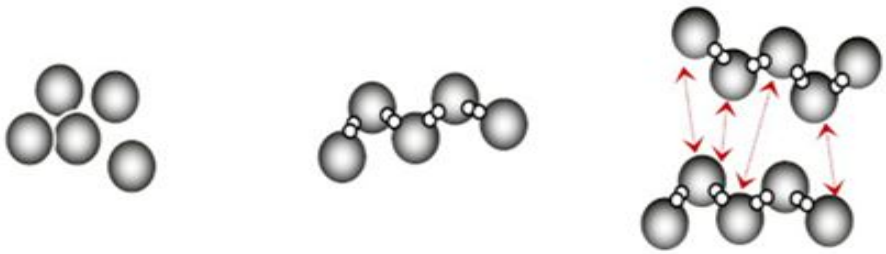

Fig. 1. A schematic description of the formation of molecules and various contributions to the Helmholtz free energy in PC-SAFT EoS [46].

In this research, in order to obtain the desired accuracy, both of the cubic equations of state (ER and PR) and molecular equation of state (PC-SAFT) were used. The PR EoS [18,19], and the ER EoS [16,17,36] were explained in details in the previous works [16-19].

The PC-SAFT EoS is a modified form of the SAFT EoS. The SAFT [27-32] is a widely used and an efficient molecular EoS which is dependent to the statistical mechanics. It was developed by extending the first-order perturbation theory proposed by Wertheim [37,38] in which the Helmholtz free energy is expanded around the free energy of a reference fluid. Therefore, the EoS is expressed as the Helmholtz free energy of a reference fluid plus the perturbation terms which correct the reference system. The reference system in the SAFT EoS was assumed as the spherical segments. Initially, Ting et al. used molecular EoS to model the precipitation of asphaltene molecules. They assumed that polar-polar interactions are not significant and the van der Waals forces can sufficiently explain the interactions between the molecules in the asphaltic crudes. Hence, they neglected the association term in the SAFT. Ting et al. also proposed how to perform fluid characterization using the PC-SAFT EoS to model asphaltene precipitation [39]. The PC-SAFT EoS is almost an important form of the SAFT EoS derived by Gross and Sadowski. They adopted the hard-chain fluid instead of the hard-sphere used in the original SAFT as the reference fluid [31]. The PC-SAFT EoS has shown the applicability in modeling the phase equilibrium of the asphaltic crude systems, hence it has received much interest in the scientific field and industry for modeling the phase equilibrium of systems including heavy molecules like asphaltene [40-44]. In the statistical thermodynamics, the EoS is usually described by the Helmholtz free energy because it is capable of describing most of the thermodynamic properties of a system. The Helmholtz free energy of a system is described by the perturbation theory as sum of two parts: (i) an unperturbed section referred to as a reference system where the only interaction between molecules is the repulsion force, and (ii) a perturbation due to the attraction forces such as dispersion interactions [45]. In the PC-SAFT EoS, the Helmholtz free energy is expressed as follows:

$$\tilde{a}^{res} = \begin{cases} \tilde{a}^{hc} & \rightarrow \text{Reference term} \\ + & \\ \tilde{a}^{disp} & \rightarrow \text{Perturbation term} \end{cases} \quad (1)$$

where $\tilde{a}$ is the reduced Helmholtz free energy and is given by:

$$\tilde{a} = \frac{A}{kNT} \quad (2)$$

In Eq. (1), the superscripts *hc* and *disp* define the hard-chain and dispersion parts in the Helmholtz free energy, respectively. In Eq. (2), the term N denotes the overall number of molecules, k is the Boltzmann constant, and T stands for the absolute temperature. Figure 1 shows a schematic description for the formation of a molecule and various parts of the Helmholtz free energy in the PC-SAFT EoS.

Finally, Eq. (1) can be converted to the following form:

$$\tilde{a}^{res} = \tilde{a}^{hs} + \tilde{a}^{chain} + \tilde{a}^{disp} \quad (3)$$

The hard-chain reference part includes the hard sphere and the chain formation contributions. The hard-chain

$$\tilde{a}^{hc} = \bar{m}\tilde{a}^{hs} - \sum_i X_i (m_i - 1) \ln g_{ii}^{hs}(\sigma_{ii}) \quad (4)$$

where $\tilde{a}^{hs}$ is the hard-sphere term of the Helmholtz free energy, m is the mean segment number, and g_{ii}^{hs} is the hard-sphere radial distribution function.

$$\bar{m} = \sum_i x_i m_i \quad (5)$$

In Eq. (5), x_i is the mole fraction of the component "i" and m_i is the number of the segments in a chain of species "i" in the mixture. The Helmholtz free energy of a hard-sphere fluid is as follows:

$$\tilde{a}^{hs} = \frac{A^{hs}}{N_s KT} = \frac{1}{\zeta_0}\left[\frac{3\zeta_1\zeta_2}{1-\zeta_3} + \frac{\zeta_2^3}{\zeta_3(1-\zeta_3)^2} + \left(\frac{\zeta_2^3}{\zeta_3^2} - \zeta_0\right)\ln(1-\zeta_3)\right] \quad (6)$$

ζ_n is defined as:

$$\zeta_n = \frac{\pi}{6}\rho\sum_i x_i m_i d_i^m \quad , n \in (0,1,2.3) \quad (7)$$

where ρ stands for the total density number of the molecules, and d_i represents the segment diameter of the component "i" which depends on the temperature. The radial distribution function is expressed as follows:

$$g_{ij}^{hs} = \frac{1}{(1-\zeta_3)} + \left(\frac{d_i d_j}{d_i + d_j}\right)\frac{3\zeta_2}{(1-\zeta_3)^2} + \left(\frac{d_i d_j}{d_i + d_j}\right)^2 \frac{2\zeta_2^2}{(1-\zeta_3)^3} \quad (8)$$

d_i, is calculated as follows:

$$d_i(T) = \sigma_i\left[1 - 0.12\exp\left(\frac{-3\in_i}{kT}\right)\right] \quad (9)$$

where σ_i denotes the segment diameter which does not depend on the temperature, and ϵ_i stands for the depth of the square well potential of component "i". Terms m_i, σ_i, and ϵ_i are the pure-component parameters describing the non-associating molecules [27-30,46].

Molecular segments can exhibit attractive forces to each other. Dispersion (London) forces are the attractive forces existing between the segments of the same chain and also the segments of unlike chains. Dispersion interactions exist whether the molecules are polar or nonpolar. In the PC-SAFT EoS, the dispersion part of the Helmholtz free energy is:

$$\tilde{a}^{disp} = -2\pi\rho I_1(\eta,\bar{m})\overline{m^2\varepsilon\sigma^3} - \pi\rho\bar{m}C_1 I_2(\eta,\bar{m})\overline{m^2\varepsilon^2\sigma^3} \quad (10)$$

$$\overline{m^2\varepsilon\sigma^3} = \sum_i\sum_j X_i X_j m_i m_j\left(\frac{\varepsilon_{ij}}{kT}\right)\sigma_{ij}^3 \quad (11)$$

$$\overline{m^2\varepsilon^2\sigma^3} = \sum_i\sum_j X_i X_j m_i m_j\left(\frac{\varepsilon_{ij}}{kT}\right)^2\sigma_{ij}^3 \quad (12)$$

In Eq. (10), η is the packing fraction (reduced density) which is equal to ζ_3. The cross parameters for unlike pair of segments, ε_{ij} and σ_{ij}, are determined by:

$$\sigma_{ij} = \frac{1}{2}(\sigma_i + \sigma_j) \quad (13)$$

and

$$\varepsilon_{ij} = \sqrt{\varepsilon_i\varepsilon_j}(1 - k_{ij}) \quad (14)$$

where k_{ij} is a binary interaction parameter (BIP) between components "i" and "j". The terms I_1 and I_2 are the integrals defined by the perturbation theory, which can be simplified into two simple power series as follows:

$$I_1(\eta,\bar{m}) = \sum_{i=0}^{6} a_i(\bar{m})\eta^i \quad (15)$$

$$I_2(\eta,\bar{m}) = \sum_{i=0}^{6} b_i(\bar{m})\eta^i \quad (16)$$

whereas a_i and b_i are related to the chain length by the following equations:

$$a_i(\bar{m}) = a_{0i} + \left(\frac{\bar{m}-1}{\bar{m}}\right)a_{1i} + \left(\frac{\bar{m}-1}{\bar{m}}\right)\left(\frac{\bar{m}-2}{\bar{m}}\right)a_{2i} \quad (17)$$

$$b_i(\overline{m}) = b_{0i} + \left(\frac{\overline{m}-1}{\overline{m}}\right)b_{1i} + \left(\frac{\overline{m}-1}{\overline{m}}\right)\left(\frac{\overline{m}-2}{\overline{m}}\right)b_{2i} \quad (18)$$

The model constants: a_{0i}, a_{1i}, a_{2i}, b_{0i}, b_{1i}, b_{2i} and further information are available in the literature [31].

Phase Stability Analysis

Stability analysis is a procedure of finding a composition that its Gibbs free energy is less than that of a single-phase mixture considering the composition of $\bar{z}$. To express this condition mathematically, a function known as the tangent plane distance (TPD) is often used. This function can be defined by the following equation:

$$\Delta G = \sum_{i=1} y_i \left[\mu_i(\bar{y}) - \mu_i(\bar{z})\right] \quad (19)$$

A phase is stable only if ΔG be positive for any sets of mole fractions at a given pressure and temperature. In this research, the stationary point method proposed by Michelsen (1982a) is used to perform the stability analysis [47]. The objective is to solve the following nonlinear equations to locate the stationary points:

$$\ln Y_i + \ln\varphi(y) - h_i = 0 \qquad i \in \{1, 2, \ldots n_c\} \quad (20)$$

where Y_i is the trial composition, and the mole fraction (y) is defined by Eq. (21).

$$y_i = \frac{Y_i}{\sum_{S=1}^{n_C} Y_S} \qquad i \in \{1, 2, \ldots n_c\} \quad (21)$$

and

$$h_i = \ln z_i + \ln\varphi(\bar{z}) \qquad i \in \{1, 2, \ldots n_c\} \quad (22)$$

The summation of variable Y is calculated for evaluating the stability of the phase resulting from the solution of Eq. (20). If this summation is larger than one, the phase is concluded to be unstable, otherwise it is considered as a stable phase.

For the sake of simplicity, we used the Rachford-Rice flash calculation method [48] (Eqs. ((24)-(26)) combined with the Wilson equation (Eq. (23)) [49] to perform flash calculation.

$$K_i = \frac{P_{ci}}{P}\exp\left(5.3727(1+\omega_i)\left(1-\frac{T_{ci}}{T}\right)\right) \quad (23)$$

$$x_i = \frac{z_i}{1 + n^v\,(K_i - 1)} \quad (24)$$

$$y_i = \frac{K_i z_i}{1 + n^v\,(K_i - 1)} \quad (25)$$

$$f(n^v) = \sum_{i=1}^{N_C}(y_i - x_i) = \sum_{i=1}^{N_C}\frac{z_i\,(K_i - 1)}{1 + n^v\,(K_i - 1)} = 0 \quad (26)$$

One of the desired and important quantities in phase equilibrium calculations is the fugacity coefficient. The fugacity coefficient could be derived from the residual chemical potential [31].

Density

It is obvious that precise calculation of the density has an important effect on the accurate modeling of the MMP. The density, ρ, can be estimated from the following relation:

$$\rho = \frac{P}{ZkT}\left(10^{-10}\frac{m}{\overset{\circ}{A}}\right)^3 \quad (27)$$

where Z is defined as follows:

$$Z = 1 + Z^{hc} + Z^{disp} \quad (28)$$

The relationship between the reduced density and the number density of the molecules is as follows:

$$\rho = \frac{6}{\pi}\eta\,(\textstyle\sum_i X_i m_i d_i^3)^{-1} \quad (29)$$

In Newton's iterations, the reduced density is updated according to the following equation:

$$\eta^{k+1} = \eta^k - \frac{p^k - p^{sys}}{\left(\frac{\partial p}{\partial \eta}\right)_{T,X}} \quad (30)$$

The partial derivatives of pressure on the basis of the

reduced density at constant temperature and composition could be calculated from Eq. (31).

$$\left(\frac{\partial p}{\partial \eta}\right)_{T,\bar{x}} = 10^3 kT\left[\rho\left(\frac{\partial Z}{\partial \eta}\right)_{T,\bar{x}} + Z\left(\frac{\partial \rho}{\partial \eta}\right)_{T,\bar{x}}\right] \quad (31)$$

Multiple Mixing-cell Model

In this contribution, the multiple mixing-cell method developed by Ahmadi and John [33], and Ahmadi [15] was used to estimate the MMP. This method compared to MOC procedures is very strong, as somehow flash calculations are in the positive composition region, so it is not necessary to use the iterative methods like the Newton-Raphson method. The procedure of this algorithm is summarized below:

1. Fixing the reservoir temperature and adjusting the initial pressure on less than that for the MMP for example 1000 psia.
2. Starting with two cells by mixing oil and gas and, moreover, flash the related composition to reach two new equilibrium compositions called x and y.
3. Combining the gained equilibrium x with equilibrium y. Each contact contributes to relate the recent compositions for the subsequent complex of contacts.
4. Keep the trend by applying more contacts with combination of the left hand-side and right hand-side cells as reported in Fig. 2, till all N_c-1 key tie lines converge with a determined connivance.
5. Computing the length of each key tie line received in the previous stage and save the minimum tie-line length (TL). Key tie-line is received when three sequential cells have a zero incline during a determined tolerance of 1.0×10^{-8}.
6. Raising the pressure and reiterating steps 4 and 5, until the MMP is specified when a single tie line becomes a critical tie line. The critical tie line is specified by filtering the near critical points and extrapolating the final two or three refined points of tie line with pressure to zero [15,33,50].

Modified Multiple Mixing-cell Model

In this study, we have modified the multiple mixing-cell algorithm outlined by Ahmadi and Johns [33]. The procedure of this modified algorithm is expressed below:

Determination of the major inputs including reservoir temperature, the number of cells, and the initial pressure as the most important parameter that must be lower than MMP.

Dividing the cells into two parts, as shown in Fig. 3, for the sake of simplicity and on the basis of the same behavior of central and side cells.

Calculating the number of cells using $N_{cell} = \frac{s(s+1)}{2}$, which "*s*" represents the number of stages (see Fig. 3). It should be noted that to prevent time-consuming calculations, we consider two cells of pre-mixed oil and gas as one cell during each contact.

We can formulate the number of left-hand side cells of triangular by $L = \frac{s(s-1)}{2} + 1$ and the right-hand side cells of triangular by $R = \frac{s(s-1)}{2} + s$.

Since the identity number of each line is equal to the summation of cells in that line, we can easily get the number of central cells by knowing the number of left-hand side cells or right hand-side cells.

In the beginning of contacts, we combine the fresh oil with gas, liquid x_e and vapor y_e resulting from flashing of these contacts.

According to the fact that this algorithm works with any number of cells, the identity number of gained equilibrium liquid (s) x_e and equilibrium vapor y_e would be fixed there, which can be obtained by $Nxe = R + n$ and $Nye = R + n + 1$, respectively, in which *n* increases during each contact one by one.

To keep contacts going until key tie lines length converged to a low tolerance (10^{-12} for cubic equations of state (PR and ER) and 10^{-3} for molecular equation of state (PC-SAFT) and retain the minimum key tie line length.

Depending on the minimum key tie line length, the pressure increases to 200 psi for tolerance of more than 10^{-3}, 1 psi for tolerance of less than 10^{-6}, otherwise 10 psi.

By reaching the tolerances of steps 8 and 9 simultaneously, the final pressure is MMP.

RESULTS AND DISCUSSION

In this research, the MMPs for cases 1-10 were calculated using the PC-SAFT together with the robust multiple mixing-cell method. Table 1 shows oil and gas

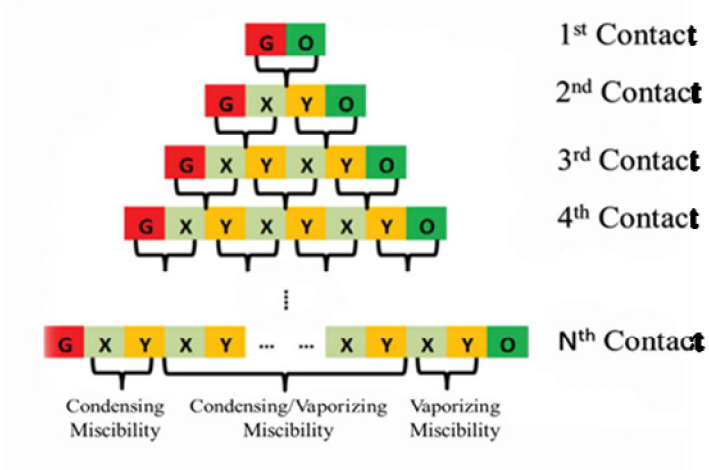

Fig. 2. Multiple mixing-cell model [26].

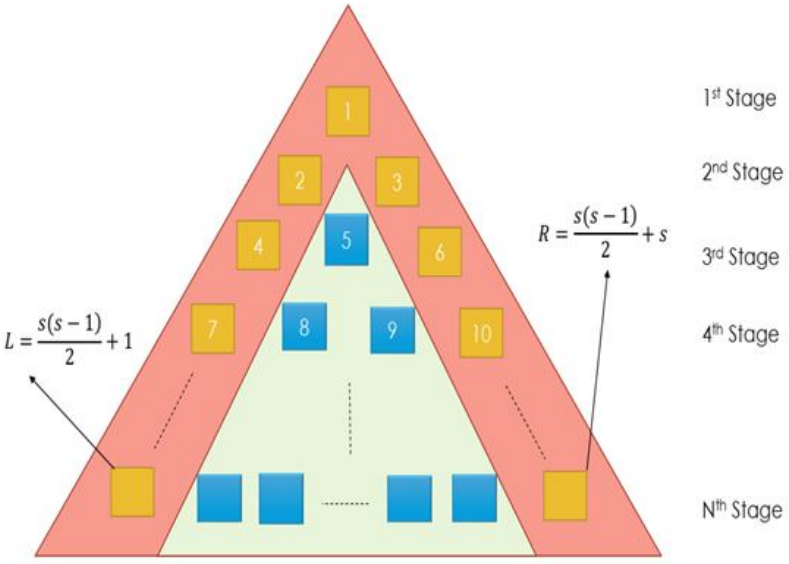

Fig. 3. Method of dividing cell into two parts.

composition reported by Esmaeilzadeh and Roshanfekr [17]. Reservoir temperature and pressure are 187.6 °F and 174.2 atm and 211.5 °F and 387.6 atm for oil A and oil B, respectively.

Table 2 presents the comparison between the experimental results of MMP measured by the VIT method, the calculated results of MMP by the Wang method coupled with the PR EoS, PT EoS, VPT EoS and the ER EoS and those obtained in this work by the multiple mixing cell method coupled with the PR EoS, ER EoS and the PC-SAFT EoS

The results of Table 2 prove that among the various couples of the mixing cell methods with different equations of state, the modified mixing cell method coupled with the PC-SAFT EoS leads to the best results (AAD% = 3.54) and using a more complicated EoS like the PC-SAFT increases the accuracy of the MMP calculation. Furthermore, coupling the modified mixing cell method with the PR EoS is the best choice among the cubic EoSs coupled with the mixing cell method.

Table 1. Oil and Gas Composition Reported by Esmaeilzadeh and Roshanfekr [17]

Component	O_A	O_B	G_A	G_B	G_C	G_D	G_E
H_2S	0.0137	-	-	-	-	-	-
N_2	0.0057	0.0015	0.0106	0.0103	0.0033	0.0029	0.0026
CO_2	0.0082	0.0069	0.0101	0.0100	0.0110	0.0123	0.0141
C_1	0.3513	0.4506	0.4693	0.4547	0.9011	0.7830	0.7032
C_2	0.1015	0.0537	0.1638	0.1661	0.0601	0.0808	0.0949
C_3	0.0695	0.0544	0.2342	0.2426	0.0209	0.0644	0.0938
IC_4	0.0101	0.0098	0.0402	0.0417	0.0012	0.0088	0.0140
NC_4	0.0316	0.0285	0.0616	0.0641	0.0021	0.0220	0.0354
IC_5	0.0229	0.0124	-	-	0.0002	0.0066	0.0109
NC_5	0.0174	0.0180	0.0101	0.0105	-	0.0071	0.0120
C_6	0.0368	0.0913	-	-	-	0.0182	0.0198
C_{7+}	0.3304	0.2729	-	-	-	-	-
M_{w7+}	205	241	-	-	-	-	-
S_{C7+}	0.8397	0.8790	-	-	-	-	-

Table 3 shows gas-condensate and gas composition reported by Esmaeilzadeh and Roshanfekr [17]. Dew Point Pressure (DPP) data and the theoretical calculation for MMP with different methods are presented in Table 4. Reservoir temperature and pressure are 227.2 °F and 220.5 atm, respectively. The calculated results of the modified mixing cell method with the PR, ER and PC-SAFT EoSs are superior to those obtained by the Wang method with the use of ER, VPT, PT and PR EoSs. Table 5 presents the oil and gas composition reported by Esmaeilzadeh and Roshanfekr [17].

The calculated MMP with different EoSs along with the experimental measurements by the slim tube method are presented in Table 6. Reservoir temperature and pressure are 184.6 °F and 103.3 atm and 184.6 °F and 206.8 atm for oil C and oil D, respectively. The results of Table 6 indicate that the coupling of modified mixing cell method with the PC-SAFT EoS presents the MMP with a higher accuracy than the other methods. The error of the modified mixing cell method coupled with the PC-SAFT EoS is much less than that of the other EoSs. Table 7 shows the oil and gas composition reported by Ahmadi-Johns [33].

The calculated MMP with different EoSs and the experimental results of MMP measured by the slim tube method are presented in Table 8. Reservoir temperatures are 160 °F and 120 °F for oil E and oil F, respectively. Table 8 shows the PC-SAFT EoS has the ability to calculate the MMP with better accuracy than the other theoretical methods. It indicates that in addition to attraction and repulsion forces, the other intermolecular forces are also important for these cases.

The calculated MMPs for 9 different cases obtained by coupling of the modified Ahmadi-Johns with the PC-SAFT, PR and the ER EoS are summarized in Table 9. Moreover, the AAD% of these methods for all of the studied cases as well as their overall AAD% are presented in Table 9.

Considering all of the cases, the minimum AAD% of the PR is 1.62 obtained for case 1, the ER EoS presents the

Table 2. Comparison between the Calculated MMP (atm) for Cases 1-5

Method	O_A-G_A	O_A-G_B	O_B-G_C	O_B-G_D	O_B-G_E	Overall
VIT[b]	146.00	138.10	620.30	570.50	313.80	
ER EoS[a]	160.00	149.50	733.20	669.10	345.50	
AAD%	9.50	8.20	18.20	14.70	10.20	12.16
PTV EoS[a]	164.30	154.50	761.70	691.00	358.80	
AAD%	12.50	11.80	22.80	21.20	14.30	16.52
PT EoS[a]	161.80	151.70	747.50	676.80	348.90	
AAD%	10.80	9.80	20.50	18.50	11.10	14.14
PR EoS[a]	125.10	117.10	449.10	421.60	263.10	
AAD%	14.30	15.20	27.60	26.00	15.90	19.80
This work, PR	143.64	142.89	653.23	653.20	326.61	
AAD%	1.62	3.47	5.31	14.50	4.08	5.79
This work, ER	153.10	156.50	643.00	646.40	336.80	
AAD%	4.86	13.32	3.66	13.30	7.32	8.49
This work, PC-SAFT	150.10	141.87	612.41	530.75	301.57	
AAD%	2.81	2.73	1.27	6.97	3.90	3.54

[a]Wang method [17]. [b]VIT data [51]. $AAD\% = \frac{\left|MMP_{cal} - MMP_{\exp}\right|}{MMP_{\exp}} \times 100$.

Table 3. Condensate and Gas Composition Reported by Esmaeilzadeh and Roshanfekr [17]

Component	C_C	G_F
N_2	0.0154	-
CO_2	0.0052	-
C_1	0.3940	1
C_2	0.0333	-
C_3	0.0227	-
IC_4	0.0072	-
NC_4	0.0131	-
IC_5	0.0083	-
NC_5	0.0079	-
C_6	0.4924	-
M_{w7+}	129.2300	
S_{C7+}	0.8120	

Table 4. Comparison between the Calculated MMP (atm) for Case 6 with Different EoSs

Method	C_C - G_F	AAD%
Experimental DPP[b]	327.60	-
ER EoS[a]	353.10	7.78
VPT EoS[a]	365.30	11.50
PT EoS[a]	355.70	8.57
PR EoS[a]	265.20	18.90
This work, PR	340.22	3.85
This work, ER	317.09	3.20
This work, PC-SAFT	313.01	4.45

[a]Wang method [17]. [b]Experimental DPP data [17]. $AAD\% = \frac{\left|MMP_{cal} - MMP_{\exp}\right|}{MMP_{\exp}} \times 100$.

Table 5. Oil and Gas Composition Reported by Esmaeilzadeh and Roshanfekr [17]

Component	O_C	O_D	G_G	G_H
CO_2	0.0449	0.0656	0.2218	0.1775
C_1	0.2071	0.3711	0.2349	0.3878
C_2	0.0481	0.0538	0.2350	0.1880
C_3	0.0409	0.0373	0.2745	0.2196
nC_4	0.0323	0.0261	0.3380	0.2710
nC_5	0.0247	0.0187	-	-
C_6	0.0298	0.0218	-	-
C_{7+} (1)	0.2525	0.1791	-	-
C_{7+} (2)	0.1285	0.0910	-	-
C_{7+} (3)	0.0855	0.0605	-	-
C_{7+} (4)	0.0631	0.0447	-	-
C_{7+} (5)	0.0427	0.0302	-	-

minimum AAD% = 3.20 for case 6, while the smallest AAD% was obtained by the PC-SAFT is 0.65 for case 9. Based on the overall AAD%, it can be simply concluded that the PC-SAFT EoS has the most accurate results compared to the other methods assessed in this work. This accuracy may be related to the versatile perturbed-chain

Table 6. Comparison between the Calculated MMP (atm) for Cases 7-8 with Different EoSs

Method	O_C - G_G	AAD%	O_D - G_H	AAD%	Overall
Slim tube[b]	152.00	-	213.80	-	
ER EoS[a]	165.40	8.81	230.30	7.71	8.26
PTV EoS[a]	171.30	12.60	237.60	11.10	11.85
PT EoS[a]	168.10	10.60	233.60	9.26	9.93
PR EoS[a]	140.20	7.76	178.60	16.40	12.08
This work, PR	176.91	16.39	204.13	4.52	10.45
This work, ER	170.11	11.91	197.30	7.71	9.81
This work, PC-SAFT	140.85	7.34	210.94	1.34	4.34

[a]Wang method [17]. [b]Slim tube data points [17]. $AAD\% = \frac{\left|MMP_{cal} - MMP_{\exp}\right|}{MMP_{\exp}} \times 100$.

Table 7. Oil and Gas Composition Reported by Ahmadi and Johns [33]

Component	O_E	O_G	G_I	G_J
CO_2	-	-	0.80	1.00
C_1	0.20	0.35	0.20	-
C_2	-	0.03	-	-
C_3	-	0.04	-	-
C_4	0.15	0.06	-	-
C_5	-	0.04	-	-
C_6	-	0.03	-	-
C_7	-	0.05	-	-
C_8	-	0.05	-	-
C_{10}	0.65	0.30	-	-
C_{14}	-	0.05	-	-

statistical associating fluid theory. Comparison the AAD% for three different methods for case 6 (gas-condensate) clearly shows that the ER EoS presents the best results.

Figure 4 shows six different profiles of the key tie-line lengths regarding to the displacement in which pressure is 2000 psia (less than MMP) against cell number for case 1. According to this figure, the three key tie lines keep boosting in accordance with the increase in number of contacts. The key tie lines are not expanded in its full sense when the number of tie lines is 10 (s = 10). The MMP in

Table 8. Comparison between the Calculated MMP (atm) for Cases 9-10 with different EoSs

Method	O_E-G_I	O_G-G_J
Slim tube exp.	1380	-
John and Orr	1466	2350
AAD%	6.23	-
Ahmadi and John	1298	2303
AAD%	5.94	-
This work, PR	1336	2296
AAD%	3.19	-
This work, ER	1337	2200
AAD%	3.11	-
This work, PC-SAFT	1370.99	2300
AAD%	0.65	-

Table 9. Summary of MMPs and AAD% for Cases 1-9

Case no.	Exp.	This work (PR EoS)	AAD%	This work (ER EoS)	AAD%	This work (PC-SAFT EoS)	AAD%
Case 1	146.00	143.64	1.62	153.10	4.86	150.10	2.81
Case 2	138.10	142.89	3.47	156.50	13.32	141.87	2.73
Case 3	620.30	653.23	5.31	643.00	3.66	612.41	1.27
Case 4	570.50	653.20	14.50	646.40	13.30	530.75	6.97
Case 5	313.80	326.61	4.08	336.80	7.32	301.57	3.90
Case 6	327.60	340.22	3.85	317.09	3.20	313.01	4.45
Case 7	152.00	176.91	16.39	170.11	11.91	140.85	7.34
Case 8	213.80	204.13	4.52	197.30	7.71	210.94	1.34
Case 9	1380.00	1336.00	3.19	1337.00	3.11	1370.99	0.65
Overall AAD%			6.32		7.59		3.49

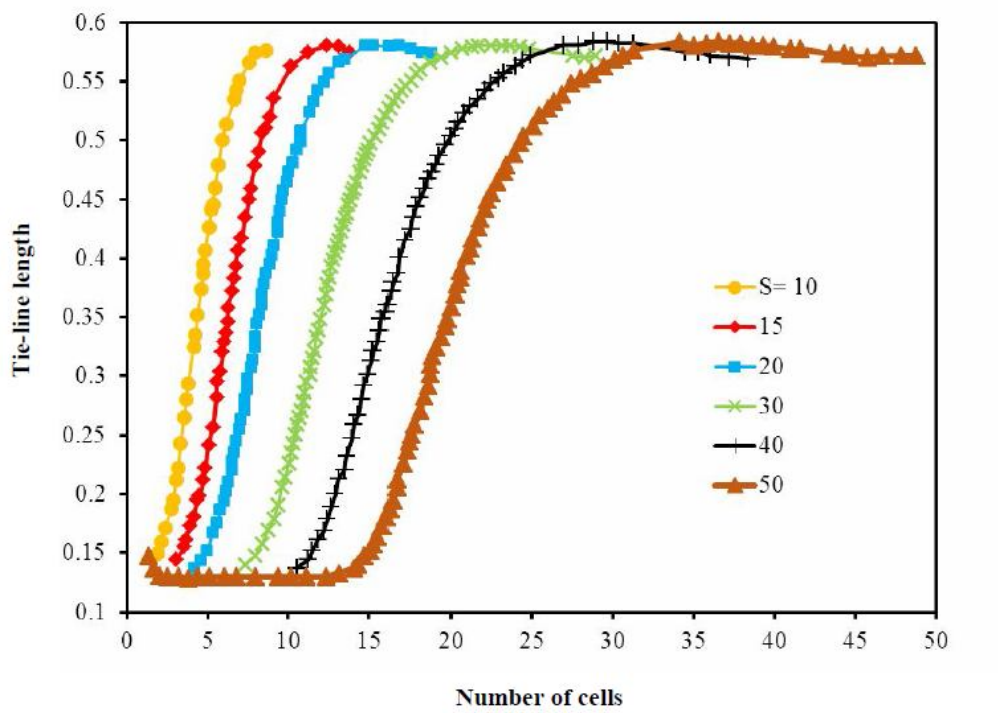

Fig. 4. Six profiles of the key tie-line length with regard to displacement in which pressure is 2000 psia (less than MMP) against the number of cells for case 1.

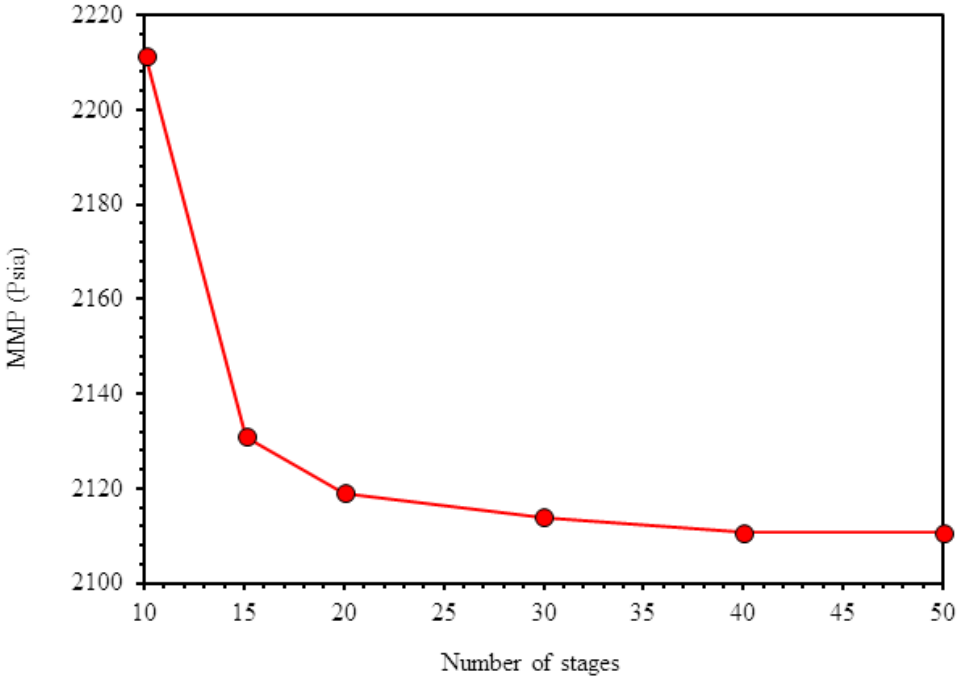

Fig. 5. Variation of the MMP *versus* the number of stages for case 1.

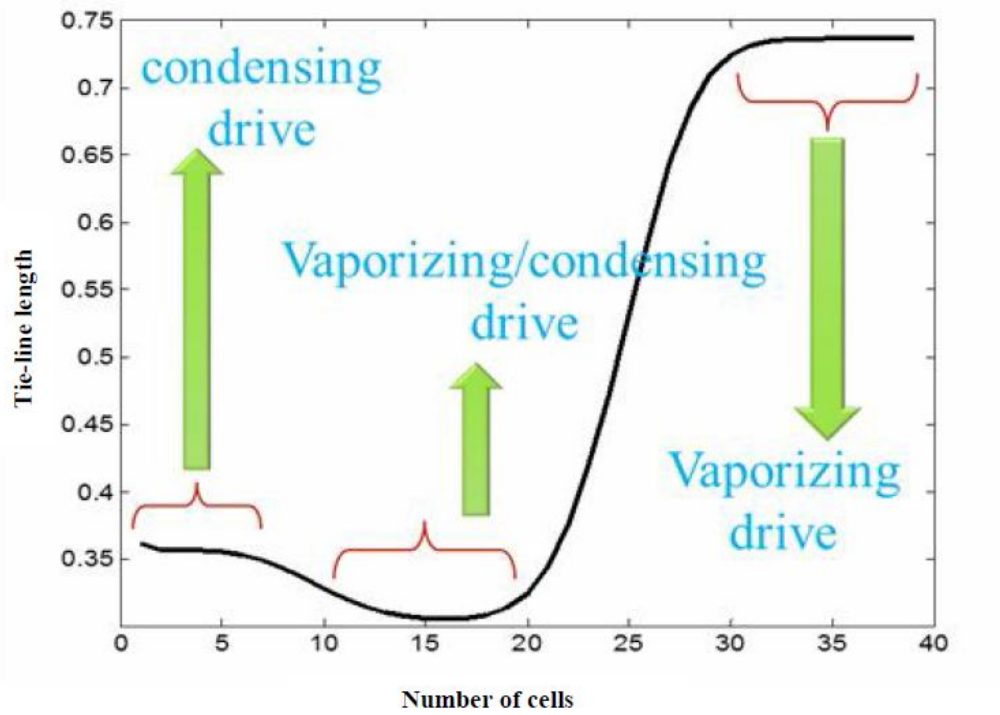

Fig. 6. Variation of tie-line length *vs*. the number of cells when vaporizing/condensing dominated (case 9 at 2000 psia).

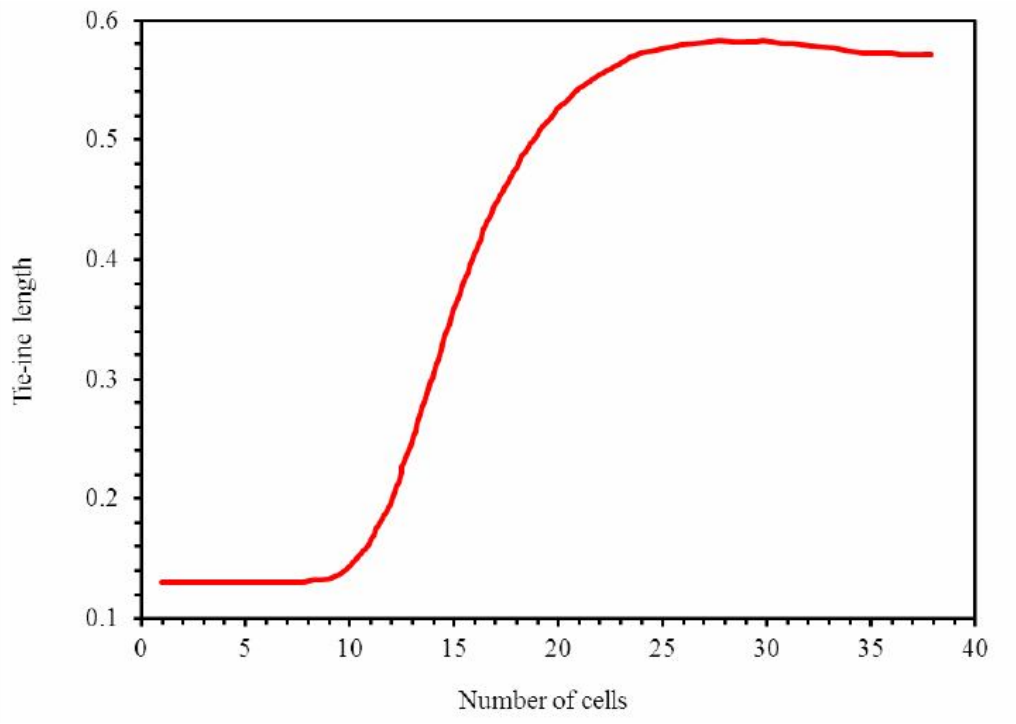

Fig. 7. Variation of tie-line length *vs*. the number of cells when condensing dominated (case 1 at 2000 psia).

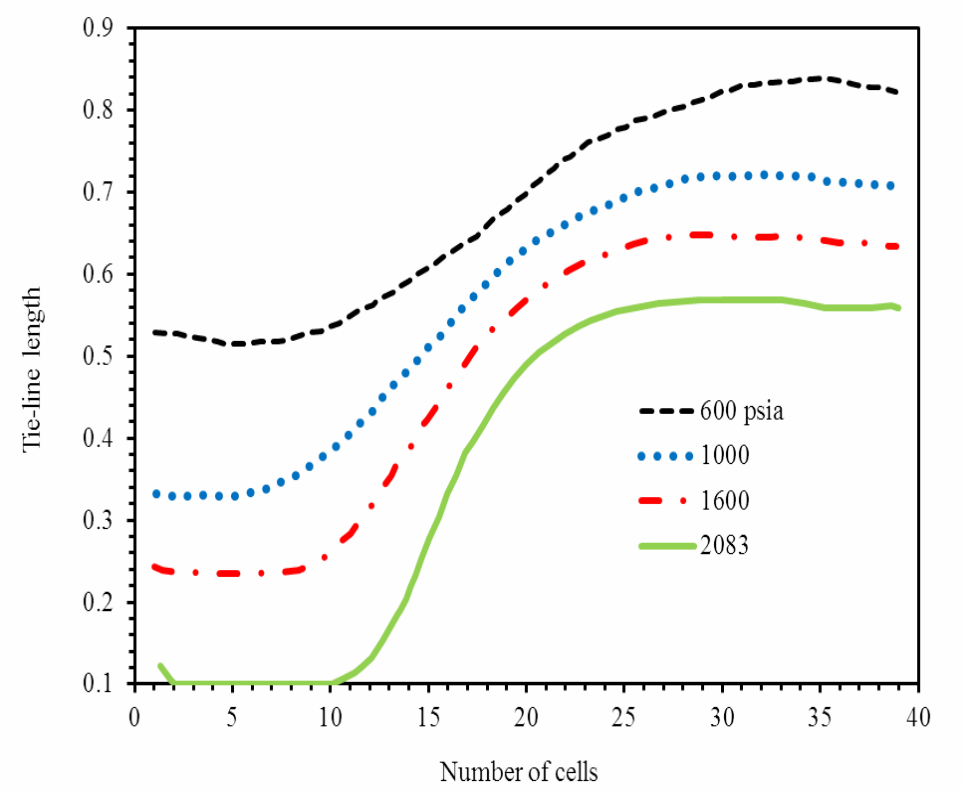

Fig. 8. Changing the condensing drive mechanism to vaporizing/condensing drive with increasing the pressure (case 1).

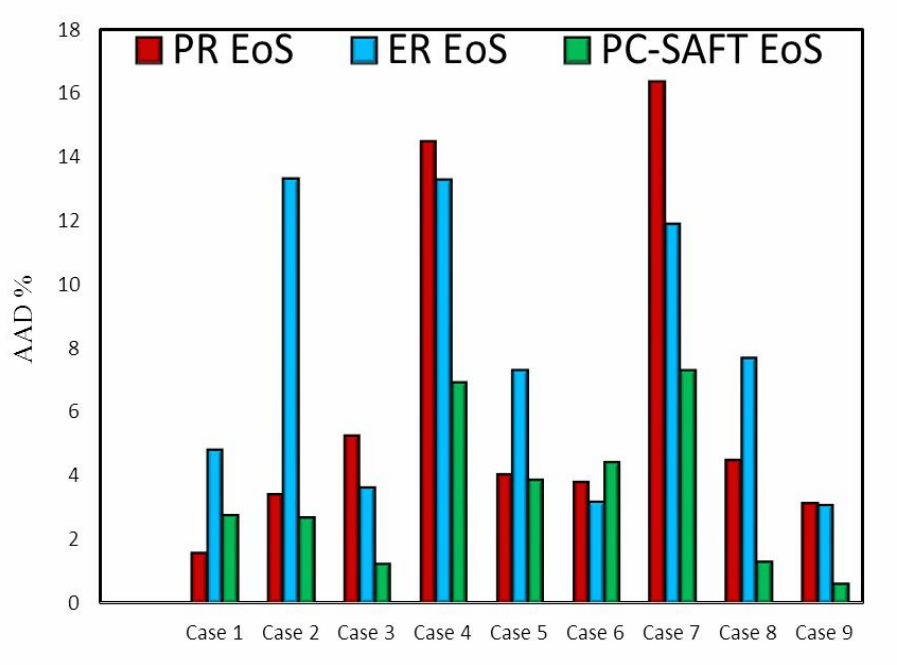

Fig. 9. Variation of AAD% of cases 1-9 for different EoSs.

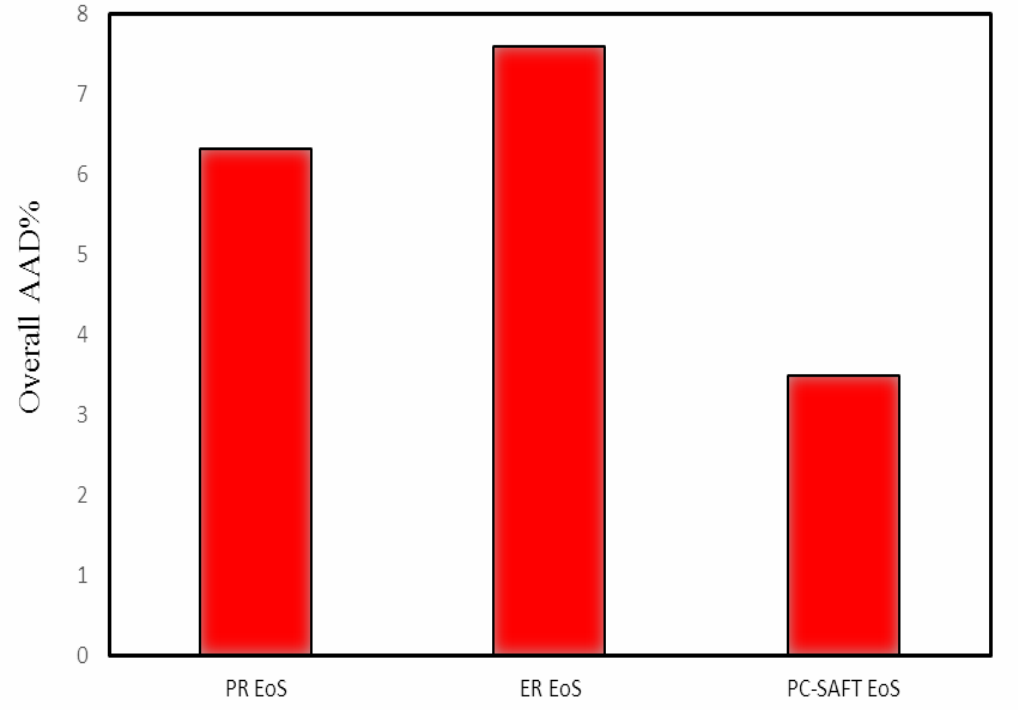

Fig. 10. Variation of overall AAD% for different EoSs.

this pressure is about 2211 psia using the PR EoS (with 4.7% error). Results indicate that with increasing the number of stages, prediction of the MMP is improved until a nearly expanded tie-line in its full sense stage (in this case, s = 40), and after this stage, tie-line length variations reached approximately zero.

Figure 5 exhibits the MMP versus the number of stages for case 1. It is obvious that the change in the MMP decreases from stage 30 and the MMP becomes approximately constant from stage 40. Figure 6 demonstrates the variation of tie-line *versus* the number of cells for case 9 at 2000 psia.

The procedure for determining the mechanism is as follows:

The variation of tie-line *versus* the number of cells is drawn, if the incipient cells have the minimum tie-line, the mechanism is then condensing, if the final cells have the minimum tie-line, the mechanism is vaporizing; finally, if the central cells have the minimum tie-line, the mechanism is vaporizing/condensing. From Fig. 6, it is concluded that the dominant mechanism is vaporizing/condensing.

Figure 7 shows the variation of tie-line versus the number of cells in case 1 at 2000 psia. Figure 7 obviously confirms that the dominant mechanism is condensing. Figure 8 presents the effect of pressure on mechanism for case 1. As can be seen, when the tie-line length increases, the mechanism of condensing drive changes to vaporizing/condensing drive. Figure 10 presents the variation of overall AAD% for different EoSs.

CONCLUSIONS

The most important results obtained in this study can be summarized as follows:

1. The multiple mixing-cell method coupled with the PC-SAFT EoS represented the most accurate results for prediction of the MMPs in most of the systems assessed in this work.

2. The overall AAD% of the PC-SAFT, PR and ER EoSs were 3.49%, 6.32% and 7.59%, respectively. It shows that the SAFT EoS can decrease the AAD of MMP calculation by about 50%.

3. The ER EoS presented the highest accuracy for the MMP for the gas condensate system.
4. The proposed algorithm makes it possible to save time especially for the cases containing a large number of components.

ACKNOWLEDGEMENTS

The authors are deeply grateful for supporting of chemical and petroleum engineering department of Shiraz University for this research.

List of Symbols

a	Attraction parameter in EoS
AAD	Average absolute deviation
b, c	Co-volume
K	Equilibrium constant
P	Pressure
R	Universal gas constant, J mol^{-1} K^{-1}
T	Temperature
x_i	Liquid mole fraction
y_i	Vapor mole fraction
Z	Compressibility factor
Z_i	Total phase mole fraction
A	Helmholtz free energy, J
a_{01}, a_{02}, a_{03}	Model constants
b_{01}, b_{02}, b_{03}	Model constants
D	A temperature-dependent segment diameter, Å
g^{hc}	Hard-chain fluid average radial distribution function
K	The Boltzmann constant, J/K
K_{ij}	Binary interaction parameter
M	The number of segments per chain
$\overline{m}$	Mean segment number
N	Total number of molecules
X	Reduced radial distance

Greek Letters

ξ_c	An empirical compressibility factor
Y	Molar volume
Ω	Acentric factor
Ω_a, Ω_b, Ω_c	Parameters of EoS
ε	Depth of pair potential, J
η	Packing fraction, $\eta = \zeta_3$
P	Total number density of molecules, $1/Å^3$
σ	Segment diameter, Å
ξ_n	Abbreviation (n = 0, ..., 3), $Å^{n-3}$

Subscripts

C	Critical point
I	ith point
J	jth point
k	kth point
N	Number of data points
r	Reduced value

Superscripts

L	Liquid
V	Vapor
Disp	Contribution of dispersive attraction
Hc	Residual contribution of hard-chain
Hs	Residual contribution of hard-sphere

REFERENCES

[1] Wang, Y.; Orr, F. M., Analytical calculation of minimum miscibility pressure. *Fluid Phase Equilib.* **1997**, *139*, 101-124, DOI: 10.1016/S0378-3812(97)00179-9.

[2] Jessen, K.; Orr, F. M., Gas cycling and the development of miscibility in condensate reservoirs. *SPE Reservoir Eval. Eng.* **2004**, *7*, 334-341, DOI: 10.2118/84070-PA.

[3] Hoier, L.; Whitson, C. H., Miscibility variation in compositionally grading reservoirs. *SPE Reservoir Eval. Eng.* **2001**, 4, 36-43, DOI: 10.2118/69840-PA.

[4] Shokrollahi, A.; Arabloo, M.; Gharagheizi, F.; Mohammadi, A. H, Intelligent model for prediction of CO_2-reservoir oil minimum miscibility pressure. *Fuel* **2013**, *112*, 375-384. DOI: 10.1016/j.fuel.2013.04.036.

[5] Haghtalab, A.; Hasannataj, H.; Panah, H. S, Prediction of minimum miscibility pressure of pure CO_2, carbon dioxide gas mixtures and polymer-supercritical CO_2 in oil using modified quadrupole Cubic Plus Association Equation of State (mqCPA EoS). *Fluid Phase Equilib.* **2018**, *478*, 114-128. DOI:

10.1016/j.fluid.2018.09.009.

[6] Gu, Y.; Hou, P.; Luo, W, Effects of four important factors on the measured minimum miscibility pressure and first-contact miscibility pressure. *J. Chem. Eng. Data* **2013**, *58*, 1361-1370. DOI: 10.1021/je4001137.

[7] Zendehboudi, S.; Ahmadi, M. A.; Bahadori, A.; Shafiei, A.; Babadagli, T., A developed smart technique to predict minimum miscible pressure-EOR implications. *The Canadian J. Chem. Engin*. **2013**, *91*, 1325-1337. DOI: 10.1002/cjce.21802.

[8] Orr, F. M.; Jessen, K., An analysis of the vanishing interfacial tension technique for determination of minimum miscibility pressure. *Fluid Phase Equilib.* **2007**, *255*, 99-109, DOI: 10.1016/j.fluid.2007.04.002.

[9] Shojaei, H.; Rastegar Moghadam, R.; Jessen, K., Experimental and Modeling Study of Multicontact Miscible Displacements. In SPE Improved Oil Recovery Symposium. Society of Petroleum Engineers, 2012. DOI: 10.2118/154307-MS.

[10] Fazlali, A.; Nikookar, M.; Agha-Aminiha, A.; Mohammadi, A. H., Prediction of minimum miscibility pressure in oil reservoirs using a modified SAFT equation of state. *Fuel* **2013**, *108*, 675-681. DOI: 10.1016/j.fuel.2012.12.091.

[11] Emera, M. K.; Sarma, H. K., A reliable correlation to predict the change in minimum miscibility pressure when CO2 is diluted with other gases. *SPE Reservoir Eval. Eng*. **2006**, *9*, 366-373, DOI: 10.2118/93478-PA.

[12] Emera, M. K.; Sarma, H. K., A genetic algorithm-based model to predict co-oil physical properties for dead and live oil. *J. Can. Pet. Technol.* **2008**, *47*, 52-61, DOI: 10.2118/08-02-52.

[13] Emera, M. K.; Sarma, H. K., Use of genetic algorithm to estimate CO_2-oil minimum miscibility pressure-a key parameter in design of CO_2 miscible flood. *J. Pet. Sci. Eng*. **2005**, *46*, 37-52, DOI: 10.1016/j.petrol.2004.10.001.

[14] Bon, J.; Emera, M. K.; Sarma, H. K., An experimental study and genetic algorithm (GA) correlation to explore the effect of nC_5 on impure CO_2 minimum miscibility pressure (MMP). SPE Asia Pac. Oil Gas Conf. Exhib., 11-13 September, Adelaide, Australia, **2006**, DOI: 10.2118/101036-MS.

[15] Ahmadi, V., Advances in Calculation of Minimum Miscibility Pressure, PhD dissertation, the University of Texas at Austin, Austin, Texas, 2011.

[16] Esmaeilzadeh, F.; Roshanfekr, M., A new cubic equation of state for reservoir fluids. *Fluid Phase Equilib.* **2006**, *239*, 83-90, DOI: 10.1016/j.fluid.2005.10.013.

[17] Esmaeilzadeh, F.; Roshanfekr, M., Calculation of minimum miscibility pressure for gas condensate reservoirs. *Fluid Phase Equilib*. **2006**, *249*, 75-81, DOI: 10.1016/j.fluid.2006.08.010.

[18] Peng, D. Y.; Robinson, D. B., A new two-constant equation of state, Ind. Eng. Chem. Fundam. **1976**, 15, 59–64, DOI: 10.1021/i160057a011.

[19] [19] Robinson, D. B.; Peng, D. Y., The characterization of the heptanes and heavier fractions for the GPA Peng-Robinson programs, Gas Processors Association, 1978.

[20] [20] Patel, N. C.; Teja, A. S. A new cubic equation of state for fluids and fluid mixtures. *Chem. Eng. Sci.* **1982**, *37*, 463-473, DOI: 10.1016/0009-2509(82)80099-7.

[21] Valderrama, J. O., The state of the cubic equations of state. *Ind. Eng. Chem. Res.* **2003**, *42*, 1603-1618, DOI: 10.1021/ie020447b.

[22] Jaubert, J. N.; Wolff, L.; Neau, E.; Avaullee L., A very simple multiple mixing cell calculation to compute the minimum miscibility pressure whatever the displacement mechanism. *Ind. Eng. Chem. Res.* **1998**, *37*, 4854-4859, DOI: 10.1021/ie980348r.

[23] Jaubert, J. N.; Arras, L.; Neau, E.; Avaullee, L., Properly defining the classical vaporizing and condensing mechanisms when a gas is injected into a crude oil. *Ind. Eng. Chem. Res.* **1998**, *37*, 4860-4869, DOI: 10.1021/ie9803016.

[24] Zhao, G. B.; Adidharma, H., Minimum miscibility pressure prediction using statistical associating fluid theory: Two- and Three-Phase systems. SPE Annu. Tech. Conf. Exhib., 24-27 September, San Antonio, Texas, USA, **2006**, DOI: 10.2118/102501-MS.

[25] Zhao, G. B.; Adidharma, H.; Towler, B.; Radosz, M., Using a multiple-mixing-cell model to study minimum miscibility pressure controlled by thermodynamic equilibrium tie lines. *Ind. Eng. Chem.*

Res. **2006**, *45*, 7913-7923, DOI: 10.1021/ie0606237.

[26] Ahmadi, K.; Johns, R. T, Multiple mixing-cell method for MMP calculations. SPE Annu. Tech. Conf. Exhib., 21-24 September, Denver, Colorado, USA, **2008**, DOI: 10.2118/116823-MS.

[27] Chapman, W. G.; Jackson, G.; Gubbins, K. E, Phase equilibria of associating fluids: chain molecules with multiple bonding sites. *Mol. Phys.* **1988**, *65*, 1057-1079, DOI: 10.1080/00268978800101601.

[28] Chapman, W. G.; Gubbins, K. E.; Jackson, G.; Radosz, M, SAFT: Equation-of-state solution model for associating fluids. *Fluid Phase Equilib.* **1989**, *52*, 31-38, DOI: 10.1016/0378-3812(89)80308-5.

[29] Chapman, W. G.; Gubbins, K. E.; Jackson, G.; Radosz, M, New reference equation of state for associating liquids. *Ind. Eng. Chem. Res.* **1990**, *29*, 1709-1721, DOI: 10.1021/ie00104a021.

[30] Chapman, W. G.; Sauer, S. G.; Ting, D.; Ghosh, A., Phase behavior applications of SAFT based equations of state-from associating fluids to polydisperse, polar copolymers. *Fluid Phase Equilib*. **2004**, *217*, 137-143, DOI: 10.1016/j.fluid.2003.05.001.

[31] Gross, J.; Sadowski, G, Perturbed-chain SAFT: An equation of state based on a perturbation theory for chain molecules. *Ind. Eng. Chem. Res.* **2001**, *40*, 1244-1260, DOI: 10.1021/ie0003887.

[32] Ting, P. D.; Joyce, P. C.; Jog, P. K.; Chapman, W. G.; Thies, M. C., Phase equilibrium modeling of mixtures of long-chain and short-chain alkanes using Peng-Robinson and SAFT. *Fluid Phase Equilib*. **2003**, *206*, 267-286, DOI: 10.1016/S0378-3812(03)00003-7.

[33] Ahmadi, K.; Johns, R. T, Multiple-mixing-cell method for MMP calculations. *SPE J.* **2011**, *16*, 733-742, DOI: 10.2118/116823-PA.

[34] Li, Y.; Johns, R. T.; Ahmadi, K., A rapid and robust alternative to Rachford-Rice in flash calculations. *Fluid Phase Equilib*. **2012**, *316*, 85-97, DOI: 10.1016/j.fluid.2011.12.005.

[35] Ahmadi, K.; Johns, R. T.; Mogensen, K.; Noman, R., Limitations of current method-of-characteristics (MOC) methods using Shock-Jump approximations to predict MMPs for complex Gas/Oil displacements. *SPE J*. **2011**, *16*, 743-750, DOI: 10.2118/ 129709-PA.

[36] Bonyadi, M.; Esmaeilzadeh, F., A modification of the alpha function (α), and the critical compressibility factor (ζ_c) in ER (Esmaeilzadeh-Roshanfekr) equation of state. *Fluid Phase Equilib*. **2008**, *273*, 31-37, DOI: 10.1016/j.fluid.2008.08.003.

[37] Wertheim, M., Fluids with highly directional attractive forces. II. Thermodynamic perturbation theory and integral equations. *J. Stat. Phys*. **1984**, *35*, 35-47, DOI: 10.1007/BF01017363.

[38] Wertheim, M., Thermodynamic perturbation theory of polymerization. *J. Chem. Phys*. **1987**, *87*, 7323-7331, DOI: 10.1063/1.453326.

[39] Ting, P. D.; Hirasaki, G. J.; Chapman, W. G., Modeling of asphaltene phase behavior with the SAFT equation of state. *Pet. Sci. Technol.* **2003**, *21*, 647-661, DOI: 10.1081/LFT-120018544.

[40] Gonzalez, D. L.; Ting, P. D.; Hirasaki, G. J.; Chapman, W. G., Prediction of asphaltene instability under gas injection with the PC-SAFT equation of state. *Energy Fuels* **2005**, *19*, 1230-1234, DOI: 10.1021/ef049782y.

[41] Gonzalez, D. L.; Hirasaki, G. J.; Creek, J.; Chapman, W. G., Modeling of asphaltene precipitation due to changes in composition using the perturbed chain statistical associating fluid theory equation of state. *Energy Fuels* **2007**, *21*, 1231-1242, DOI: 10.1021/ef060453a.

[42] Gonzalez, D. L.; Vargas, F. M.; Hirasaki, G. J.; Chapman, W. G., Modeling study of CO_2-induced asphaltene precipitation. *Energy Fuels* **2007**, *22*, 757-762, DOI: 10.1021/ef700369u.

[43] Panuganti, S. R.; Vargas, F. M.; Gonzalez, D. L.; Kurup, A. S.; Chapman, W. G., PC-SAFT characterization of crude oils and modeling of asphaltene phase behavior. *Fuel* **2012**, *93*, 658-669, DOI: 10.1016/j.fuel.2011.09.028.

[44] Vargas, F. M.; Gonzalez, D. L.; Hirasaki, G. J.; Chapman, W. G., Modeling asphaltene phase behavior in crude oil systems using the perturbed chain form of the statistical associating fluid theory (PC-SAFT) equation of state. *Energy Fuels* **2009**, *23*, 1140-1146, DOI: 10.1021/ef8006678.

[45] Barker, J. A.; Henderson, D., Perturbation theory and equation of state for fluids. A successful theory of liquids. *J. Chem. Phys.* **1967**, *47*, 4714-4721, DOI:

10.1063/1.1701689.

[46] Mohebbinia, S., Advanced equation of state modeling for compositional simulation of gas floods, PhD Thesis, University of Texas, 2013.

[47] Michelsen, M. L., The isothermal flash problem. Part I. Stability. *Fluid Phase Equilib*. **1982**, *9*, 1-19, DOI: 10.1016/0378-3812(82)85001-2.

[48] Rachford, H.; Rice, J., Procedure for use of electronic digital computers in calculating flash vaporization hydrocarbon equilibrium. *J. Pet. Technol*. **1952**, *4*, 19-13, DOI: 10.2118/952327-G.

[49] Wilson, G. M., A modified Redlich-Kwong equation of state, application to general physical data calculations, in: 65th National AIChE Meeting, Cleveland, OH, 1969.

[50] Teklu, T. W.; Ghedan, S. G.; Graves, R. M.; Yin, X., Minimum Miscibility Pressure Determination: Modified Multiple Mixing Cell Method, in: SPE EOR Conference at Oil and Gas West Asia, Society of Petroleum Engineers, 2012, DOI: 10.2118/155454-MS.

[51] Ayirala, S.; Rao, D.; Casteel, J., Comparison of minimum miscibility pressures determined from gas-oil interfacial tension measurements with equation of state calculations. SPE Annu. Tech. Conf. Exhib. 5-8 October, Denver, Colorado, 2003, DOI: 10.2118/84187-MS.